TOXICOLOGICAL SCIENCES **99(1)**, 303–314 (2007)
doi:10.1093/toxsci/kfm151
Advance Access publication June 8, 2007

Estrogenic Effects in the Immature Rat Uterus after Dietary Exposure to Ethinylestradiol and Zearalenone Using a Systems Biology Approach

Marjoke Heneweer,*[,1] René Houtman,† Jenneke Poortman,* Maria Groot,* Chris Maliepaard,‡[,2] and Ad Peijnenburg*

**RIKILT – Institute of Food Safety, Wageningen UR, 6700 AE Wageningen, The Netherlands; †Pamgene International BV, 5200 BJ's-Hertogenbosch, The Netherlands; and ‡Biometris, Wageningen UR, 6700 AC Wageningen, The Netherlands*

Received May 1, 2007; accepted May 29, 2007

Residues of illegally used hormones are regularly detected in animal products, feed, or cocktails recovered at farms. In order to better understand the effects of dietary exposure to ethinyl estradiol (EE2, 0.03–1 μg/kg body weight [bw]) and zearalenone (ZEA, 0.03–1 mg/kg bw), an immature rat uterotrophic assay was performed and effects were studied at morphological, histological, and gene expression levels. Ligand-mediated coregulator recruitment by estrogen receptor α (ERα) was studied *in vitro*. Uterine weight and epithelial cell height were increased dose dependently after a 3-day oral exposure of rats to the highest tested doses of EE2 or ZEA, respectively. At low doses 0.03 μg/kg EE2 and 0.1 mg/kg ZEA, edema, and vacuolization could already be observed in some animals. Exposure to 1 mg/kg ZEA resulted in severe damage of the uterine epithelial layer. Our study suggests similar coregulator recruitment and gene expression patterns for the two estrogenic compounds. Main regulated pathways were remodeling of extracellular matrix, alternative complement activation, cell proliferation, and estrogen-mediated calcium signaling. The level of regulation differed between EE2 and ZEA, attributing a much lower estrogenic potency to ZEA than to EE2. A major difference was their ability to recruit coregulator inhibitor of kappa B beta and induce expression of the matrix metalloproteinase 7 gene (381.4- and 6.9-fold upregulation by EE2 and ZEA, respectively), which plays an important role in the maintenance of the integrity of the epithelial layer of the uterus during proliferation and growth. This observation may explain the observed differences at the histological level.

Key Words: **estrogens; DNA microarrays; coregulator peptide recruitment; rat uterus; ethinyl estradiol; zearalenone; systems biology.**

Estrogens are steroid hormones eliciting various effects, in many cells and tissues including the reproductive system, liver, muscle, and the immune system (Hall *et al.*, 2001; Nilsson *et al.*, 2001). In mammals, two intracellular nuclear estrogen receptors (ERs), ERα and ERβ, mediate the actions of estrogens via ligand-dependent processes (Klinge, 2001; Nilsson *et al.*, 2001). Two subtypes ERα and ERβ differ in their C-terminal ligand-binding domain (LBD), N-terminal transactivation domain, as well as in function, tissue-distribution and ligand-binding affinities for 17β-estradiol and estrone (Kuiper *et al.*, 1998). These observations could account for the differences in effects in different tissues after exposure to endogenous estrogens or exogenous estrogenic compounds, such as certain agrochemicals, phytochemicals, and mycotoxins. In the uterus, ERα is the predominant isoform (Wang *et al.*, 1999). After binding of the ligand to the ER, the ER undergoes a conformational change, which enables alteration of LxxLL-mediated interaction of ER with coregulator molecules, translocation of the ER from cytosol to nucleus, and subsequent binding to ER-responsive elements (Edwards, 2000; Lonard and O'Malley, 2006; Nettles and Greene, 2005).

The latter phenomenon initiates transcription of specific genes and physiological responses in target tissues. Estrogen-mediated physiological responses include maintenance and development of secondary female sex characteristics, uterotrophy, growth, and mineral density of the bone, suppressed immune function and, specifically in ruminants anabolic effects on muscle tissue (Lone, 1997; Meyer, 2001).

Residues of hormones are regularly detected in animal products, feed, or cocktails recovered at farms and therefore, diet can be considered as a consistent source of (low dose) exposure to synthetic and natural endocrine disrupting compounds, mainly found in products such as milk, eggs, and meat. A recurrent question is at which levels these hormones impose a risk to human consumers. In particular, the developing child is thought to be at increased risk since endogenous production of hormones is still at a relatively low level, and therefore this lifestage may be more susceptible to hormonal influence. ZEA is a nonsteroidal estrogenic mycotoxin produced by several *Fusarium* spp. and is found worldwide in cereal crops. The highest ZEA level was found on raw maize, reaching up to 627

[1] Current address: Laboratory of plant breeding, Wageningen UR, PO Box 386, 6700 AJ Wageningen, The Netherlands.

[2] To whom correspondence should be addressed at Bornsesteeg 45, 6708 PD Wageningen, The Netherlands. Fax: +31-317-417717. E-mail: Marjoke.Heneweer@wur.nl.

μg/kg (Eriksen *et al*., 2000). The average daily intake of ZEA, based on calculations with mean levels in the most important foods and their consumption rates, ranged from 0.8 to 29 ng/kg body weight (bw) among adults. For small children, daily intakes ranges from 6 to 55 ng/kg bw/day (Minervini *et al*., 2005). Synthetic ethinyl estradiol (EE2) and ZEA are both ERα ligands and previous *in vitro* studies have shown that EE2 and ZEA elicit similar effects, although ZEA has a lower efficacy and a 1000-fold lower potency than EE2 (Bovee *et al*., 2004). However, increasing indications that exposure to different estrogenic compounds results in compound-specific effects on morphological, histological, and molecular level (Katzenellenbogen *et al*., 1996; McDonnel and Norris, 1997; Watanabe *et al*., 2003), triggered us to further explore these observations.

The advent of the -omics technologies enables dissection of biological processes at a detailed molecular level. Therefore, in more recent studies, an *in vivo* approach was complemented with -omics data to study effects of estrogens in more detail (Daston and Naciff, 2005; Fertuck *et al*., 2003; Naciff *et al*., 2003). Alterations in processes, such as gene expression and coregulator recruitment are considered to precede and to be the basis for histological and physiological changes, and thus phenotype (Nuwaysir *et al*., 1999; Steiner and Anderson, 2000). Therefore, combination of transcriptomics, proteomics, *in vitro* and *in vivo* data (systems biology) could result in better understanding these complex biological processes. A major challenge in application of transcriptomics to the field of toxicology and endocrine disruption is to link altered gene expression levels to gross physiological changes, such as increased uterine weight, and more subtle histological changes, such as increase in uterine epithelial cell height. This process is often referred to as phenotypic anchoring of DNA microarray data (Currie *et al*., 2005).

The present study describes a rat uterotrophic assay, which quantifies increase in uterine weight upon exposure of the animal to estrogenic substances. In recent years, this protocol has been improved by integration of histological parameters, such as epithelial cell height, thereby increasing the number of uterine-based endpoints. In order to get a better understanding of the underlying mechanisms of dietary estrogen exposure, effects studied at the level of morphology and histology, were complemented by gene expression data and coregulator recruitment. We attempted to combine observed effects into a model by which phenotypes can be explained.

MATERIALS AND METHODS

Animals. Pregnant Sprague–Dawley rats were obtained from Harlan (Horst, The Netherlands) and observed for overt signs of ill health. Animals were kept at a housing temperature of approximately 22°C and at a relative humidity of 30–70%. Lighting cycle was 12-h light and 12-h dark. Animals were provided with phytoestrogen-free RMH-B feed (Arie Blok, Woerden, The Netherlands) and tap water *ad libitum*. Young rats were weaned, weighed and the female animals were allocated to treatment groups at postnatal day 21. The protocol was approved by the ethical committee for animal experiments at Wageningen University, Wageningen, The Netherlands.

Treatment. An immature rat uterotrophic assay was performed using the validated Organisation for Economic Co-operation and Development protocol as described previously (Kanno *et al*., 2003). The parameters examined were body- and organ weight and histological endpoints, such as epithelial cell height. Furthermore, in order to look for a molecular base for the observed phenotypes, coregulator recruitment and gene expression levels were studied.

For each individual animal, doses were calculated daily. Treatment groups (four rats per group) were 0 – 0.03 – 0.1 – 0.3 – 1 – 10 μg/kg bw EE2 (Steraloids, Newport, RI) and 0 – 0.03 – 0.1 – 0.3 – 1 – 10 mg/kg bw zearalenone (ZEA) (Sigma, Zwijndrecht, The Netherlands). The control group received only the vehicle ethanol (70%, 0.3 μl/g bw) (Merck, Roden, The Netherlands). EE2 and ZEA were dissolved in ethanol and mixed with 1 ml of custard. Animals were housed individually during feeding, in order to monitor whether the entire test compound was ingested. Exposure started at postnatal day 21 and lasted for 3 consecutive days. At day 4, animals were weighed and sacrificed by bleeding under isoflurane anesthesia. The doses used in this study were chosen based on previously carried out dose-finding experiments and a yeast-based reporter gene assay. Furthermore, initial dose-range finding experiments showed that concentrations above 10 μg/kg bw for EE2 and 10 mg/kg bw for ZEA did not result in higher relative uterus weights (results not shown). Comparison of the lowest dose level for ZEA used in our study with the estimated realistic human exposure levels described above shows that the realistic human exposure levels are approximately three orders of magnitude lower than the observed lowest observed effect level (LOEL) for gene expression in our study.

Organ weights. Uterine horns were dissected and trimmed of fascia and fat. Luminal fluids were expressed by gentle pressure on moistened filter paper, after which the uterus was weighed (blotted weight). Uterine weights of individual rats were divided by their respective body weights at the day of sacrifice. In order to make sure a larger uterine weight was due to treatment and not to larger body weight, analysis of covariance (ANCOVA) was performed, using the Excel (version 2003, Microsoft, Seattle, WA) add-in Xlstat-PRO version 7.5.3 (AddinSoft, New York, NY).

Histology. From each rat, one uterine horn was snap-frozen in liquid nitrogen and saved at −80°C until RNA isolation. The other horn was fixed in formalin for later use. Uteri were embedded in paraffin for histological examination. Epithelial cell height, as an indicator for cellular hypertrophy, was calculated by averaging the cell height of three locations on the hematoxylin and eosin (HE)–stained coupes for each individual animal. Statistical significance was calculated with one-way ANOVA and Dunnet's multiple comparisons test using Prism 4 (GraphPad Software Inc, San Diego, CA). Pearson's correlations between uterine weight and uterine epithelial cell height were calculated using Excel (version 2003, Microsoft).

RNA isolation. Uteri were taken from −80°C and homogenized in 1 ml of TRIzol (Invitrogen, Breda, The Netherlands) per 50–100 mg tissue, using a homogenizer (Pro Multi-Gen 7, PRO Scientific, Oxford, CT). Subsequently, RNA was isolated following supplier's instructions. After purification using the RNeasy Mini Kit (Qiagen, Venlo, The Netherlands), integrity, purity, and concentration were assessed by gel electrophoresis and spectrophotometrically at wavelengths of 230, 260, and 280 nm.

Preparation of labeled cRNA and microarray hybridization. One microgram of each individual RNA sample was amplified using a low RNA Input Fluorescent Linear Amplification Kit (Agilent Technologies, Amstelveen, The Netherlands). Subsequently, the common reference sample, i.e., a pool of all RNAs, was labeled with Cy3 and the individual RNAs of each of the treated and control animals were labeled individually with Cy5. The labeled cRNA was purified (QIAquick spin columns, QIAGEN, Venlo, The Netherlands) and 1 μg of each sample was hybridized to 44K whole genome 60-mer rat oligo microarrays (G4130A, Agilent) according to manufacturer's instructions (In situ hybridization kit plus, 5184-3568, Agilent, Amstelveen, The Netherlands). After a 17-h incubation period, slides were washed using various dilutions of SSPE (sodium chloride, sodium phosphate, EDTA) buffer according to

protocol provided by Agilent. Fluorescent images were obtained with a Scanner Array Express HT microarray scanner at 543 nm for Cy3 and 633 for Cy5 using Scan Array Express 3.0 (PerkinElmer Life and Analytical Sciences, Inc., Wellesley, MA).

Analysis of gene expression data. Spot intensities were quantified using ArrayVision 8.0 (Amersham Biosciences Niagara, Inc., St Catharines, ON, Canada). Subsequently, quality control was performed with R, using the limmaGUI interface. Signals were corrected for background and corrected data were normalized and corrected for random and systematic error (Pellis *et al.*, 2003) in Genemaths XT (Applied Maths, Sint-Martens-Latem, Belgium). In order to identify differentially regulated genes, one-way ANOVA was performed to test for differences between groups and to obtain information about within-group and between-group variability for each gene. Subsequently, separate *t*-tests were performed for each treatment group compared to the control group, using the pooled estimate of within-group variability and the appropriate degrees of freedom (both obtained from the ANOVA).

In order to correct for multiple testing, the false discovery rate (FDR) (Benjamini and Hochberg, 1995) was used, generating adjusted p values (also q values). The level for the FDR was set to $q < 0.001$.

Affected pathways were analyzed with MetaCore version 3.2.0 (GeneGo, Inc, St Joseph, MI). Functions of individual genes were retrieved using NCBI's nucleotide database.

Confirmation of gene expression data by quantitative reverse transcriptase polymerase chain reaction. Quantitative reverse transcriptase–polymerase chain reaction (RT-PCR) was used to verify selected responses in uterine tissue collected within the same animal experiment. RNA from two randomly chosen animals per treatment group, was isolated as described before and subsequently treated with DNAse I (Promega, Leiden, The Netherlands). Complementary DNA (cDNA) was synthesized using 1 μg of RNA and the iScript cDNA Synthesis Kit, following supplied instructions (Biorad, Veenendaal, The Netherlands). Eighty microliters of water was added to the obtained cDNA, which was stored at −20°C until further analysis. A PCRmix was made containing 24.5 μl of IQ Supermix, 0.4μM each of forward and reverse primer, and 9.5 μl of water per sample. For the PCR, 1 μl of cDNA of each sample was added to 24 μl of PCRmix. For each primer pair a sample that was not reverse transcribed was included in the analysis. Primers (Table 1) were selected using Beacon Designer 5 (PREMIER Biosoft International, Palo Alto, CA) in order to obtain an intron-spanning amplicon of ~200-bp length with a T_m of 60°C. After primer design, all primers were run through National Center for Biotechnology Information (NCBI) Blast (nucleotide nonredundant database) in order to check for specificity.

Acidic ribosomal phosphoprotein P0 (ARBP) was selected as reference gene as its expression levels, based upon microarray data analysis, varied between 0.9 and 1.1 in all samples. Expression levels of all genes were normalized using the ARBP-expression levels in individual samples, using a standard curve.

In vitro *ERα-coregulator interaction assay.* Ligand-modulated interaction of coregulators with ERα was assessed using PamChip peptide microarrays (PamGene, 's-Hertogenbosch, The Netherlands). In short, after binding of the ligand to the ERα, the ERα undergoes a conformational change, which leads to alteration of the interaction and association with coregulator molecules, via the so-called nuclear receptor-boxes with a conserved LxxLL-motif. Forty-eight peptides representing a selection of coregulator-derived LxxLL-motifs and modifications thereof (Table 2) were synthesized with an additional N-terminal cysteine (JPT, Berlin, Germany). 96-Array PamChips were manufactured by peptide immobilization using Piezzo technology and Pamgene proprietary thiol-based surface chemistry. Experiments were performed on a PamStation96 instrument (PamGene). This integrated peptide microarray platform enables automated multistep measurement protocols, including blocking, sample incubation by repeated passage of the sample back and forth (cycle) through the 3-dimensional porous array solid phase, washing, and image capture of up to 96 samples (arrays) in parallel.

In short, the arrays were incubated with glutathione-S-transferase (GST)-tagged human ERα-LBD (ERα-LBD-GST, Invitrogen, Breda, The Netherlands) and ligand. Nuclear receptor (NR)-coregulator peptide interaction was quantified using Alexa488-conjugated anti-GST rabbit polyclonal antibody (α-GST-Alexa488, Invitrogen).

2×-Concentrated solutions of ligand and ERα-LBD-GST + α-GST-Alexa488 were prepared in reaction buffer in advance (20mM Tris, pH 7.5, 500mM NaCl, 0.2% bovine serum albumin [BSA], 0.05% Tween-20). At the start of the experiment, 2× ligand and 2× NR/Ab were mixed 1:1 in a 96-well masterplate and incubated for 15 min on ice. During this period, the PamChip was incubated for 10 cycles using blocking buffer (20mM Tris, pH 7.5, 500mM NaCl, 1% BSA, 0.01% Tween-20). Subsequently, the blocking buffer was removed and the assay mixes were transferred to the PamChip using a multi channel pipette. Dilution series of EE2 and ZEA started at 4×10^{-6} and 4×10^{-4}M (assay concentration), respectively, using threefold serial dilution and 11 concentrations per ligand. Experiments were performed in duplo, ERα-LBD-GST and α-GST-Alexa488 assay concentrations were 20 and 25nM, respectively, and the dimethyl sulfoxide concentration in all reaction assay mixes was 2%. The assay was performed at 30°C, applying one cycle per minute, and monitored by image capture every 20 cycles. After 80 cycles, the reaction mixture was removed, the arrays were washed by three cycles using TBS/0.05% Tween-20, and Tiff images were captured.

Peptide array analysis. Image analysis was performed using BioNavigator software (Pamgene International), which performs automated array grid finding and subsequent quantification of signal and local background for each individual peptide. Raw values of spot signal minus local background were exported to GraphPad Prism (v 4.02, GraphPad Software, Inc.). Nonlinear regression was performed for a sigmoidal concentration-response curve (variable slope), without use of any constraints, initial values or weighting. Ligand-induced deltas of ERα binding per peptide were calculated using top minus bottom values of the fitted curve. SD_{top} and SD_{bottom} were calculated from the respective 95% confidence intervals of the fitted top and bottom. Effects were only accepted as being significant (*), if (top minus $3 \times SD_{top}$) > (bottom plus $3 \times SD_{bottom}$) and with EC_{50} values (logM) between −4.5 and −9.5.

TABLE 1
Primers Used for Quantitative RT-PCR

Gene	RefSeq	Oligo sequence (5′ → 3′) Sense	Oligo sequence (5′ → 3′) Anti-sense
ARBP	NM_022402	CCTAGAGGGTGTCCGCAATGTG	CAGTGGGAAGGTGTAGTCAGTCTC
APLN	NM_031612	TCTCACCCACCAAGTTCCTCTAATG	GGTCTCCAAGGGCAGTCCAAG
AQP5	NM_012779	CCGCTTTGGAATCAGGCAGAATG	TGGCACTTGAGATACTGGGTTGG
CASP7	NM_022260	GACCAGCCTCCAACTGAGAACC	GAACTCCCTCCCTGAATCAATATACTTTC
C2	NM_172222	CCACCAATCCCATCCAGAAGAGG	TGAGAGGCATCAAGCAGCAGATAG
MVD	NM_031062	CCGCCCATCTCCTACCTCAATG	CACGGTGTCCTCCAGAGTGAAG
SPP	NM_012881	GTATCCCGATGCCACAGATGAGG	TCTGCTTATACTCCTTGGACTGCTC
Calb3	NM_031984	TAGGATTCAATCAGTAGGTGGTGTCG	GATAAGAACGGTGATGGAGAAGTTAGC

TABLE 2
Coregulator Motifs Used on PamChip Peptide Microarrays

NURSA	LxxLL-peptide	SwissProt (human)	Synonyms							
ASC-1	LxxLL161_149_171_C171S	Q15650	TRIP4							
CBP	LxxLL70_57_80	Q92793								
	LxxLL358_345_368_C367S									
	LxxLL2067_2055_2077									
DAX1	LxxML13_1_23	P51843								
	LxxML80_68_90_C69S									
	LxxLL146_136_159									
NCOA-1	LxxLL633_620_643	Q15788	SRC-1	RIP160	Hin-2protein					
	LxxLL690_677_700									
	LxxLL749_737_759									
NCOA-2	LxxLL641_628_651	Q15596	GRIP1	TIF2						
	LxxLL690_677_700									
	LxxLL745_733_755									
	LxxLL878_866_888									
NCOA-3	LxxLL113_102_123_N-KKK	Q9Y6Q9	SRC-3	CIP	A1B1	ACTR	Ch-TOG	pCIP	RAC3	TRAM1
	LxxLL621_609_631									
	LxxLL621_609_631_C627S									
	LxxLL685_673_695									
NCOA-6	LxxLL887_875_897	Q14686	RAP250	Nrap250	PRIP					
	LxxLL1491_1479_1501									
NCOR	LxxHI2051_2039_2061	O75376	NCOR1							
	LxxHI2051_2039_2061_C2056S									
	LxxII2263_2251_2273									
	LxxLL2051_2039_2061									
PCAF	PCAF_LxxLL190_178_200	Q92831	P/CAF							
p300	LxxLL81_69_91	Q09472	EP300							
PGC-1	LxxLL144_130_155	Q9UBK2	PRGC1							
RIP140	LxxLL133_121_143	P48552	NRIP1							
	LxxLL185_173_195									
	LxxLL185_173_195_C177S									
	LxxLL380_368_390									
	LxxLL500_488_510									
	LxxLL713_701_723									
	LxxLL819_805_831									
	LxxLL936_924_946									
	LxxLL936_924_946_C945S									
SMRT	LxxHI2135_2123_2145	Q9Y618	NCOR2	SMAP270	TRAC					
	LxxII2342_2330_2352									
SNURF	LxxLL21_9_31_C9S_C11S	Q15466	RNF4	SHP						
	LxxIL118_106_128									
TRAP220	LxxLL604_591_614	Q15648	TRIP2	PPRB	ARC205	DRIP205	PBP	DRIP		
	LxxLL645_632_655									
TRIP3	ZNHI3_LxxLL101_89_111	Q15649	ZNHI3	HNF-4a coactivator						
TRIP5	LxxLL845_833_855_C855S	P52732	KIF11	EG5	HKSP	KNSL1				
TRIP8	LxxLL37_25_47	Q15652	JMJD1C							
TRIP9	LxxLL74_62_84	Q15653	IKBB	IkappaB-beta						
	LxxLL289_277_299									

Note. First column indicates coregulator names based on NURSA (Nuclear Receptor Signaling Atlas).

RESULTS

Uterotrophic Assay and Histology

Dietary exposure of the rats to increasing doses of EE2 or ZEA for 3 consecutive days resulted in a dose-dependent 3.9- and 2.1-fold increase of the relative uterine weight at the highest tested dose for EE2 and ZEA, respectively (Fig. 1). ANCOVA analysis showed that the observed increase of uterine weight was due to treatment and not to increase of body weight (data not shown). The LOEL corresponded to 1 μg/kg bw for EE2 and 1 mg/kg bw for ZEA (Fig. 1).

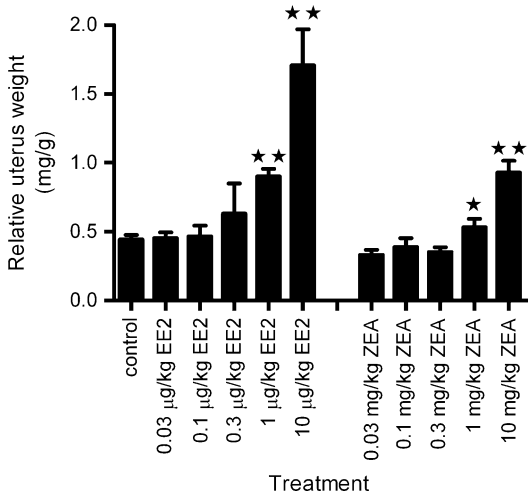

FIG. 1. Uterotrophic response expressed as relative uterus weight (uterus weight [mg]/bw [g]) in female Sprague–Dawley rats after a 3-day dietary exposure to EE2 and ZEA. Bars (mean ± SD) represent data of four animals. (*) Significantly different from control ($p < 0.05$). (**) Significantly different from control ($p < 0.0001$).

Microscopic evaluation of the HE-stained uterus sections showed that high doses of EE2 and ZEA caused increasing thickness of the epithelial layer. Analysis of uterine epithelial cell height of the individual animals resulted in a 4.0- and 2.1-fold increase after dietary exposure to the highest doses of EE2 and ZEA, respectively (Fig. 2). Statistically significant LOELs were 10 and 10 mg/kg for EE2 and ZEA, respectively. With respect to EE2 and ZEA treatment, plotting uterine weight and uterine epithelial cell height resulted in a combined Pearson's correlation $r = 0.89$. If calculated for the individual test compounds, r was 0.92 and 0.70 for EE2 and ZEA, respectively (Fig. 3).

At doses as low as 0.03 µg/kg EE2 and 0.1 mg/kg ZEA, edema and vacuolization could be observed in some animals. Where EE2 did not cause significant destruction of the epithelial layer, exposure to ZEA did result in extensive degeneration and necrosis of the epithelial cells in the uterus at concentrations higher than 1 mg/kg (Fig. 4).

Gene Expression Levels

The number of genes that were significantly regulated in rats exposed to EE2 was larger than in rats exposed to ZEA (Table 3). After ANOVA, genes that were significantly up- or downregulated with a q value < 0.001 in at least one dose group were selected. Using this criterion EE2 upregulated 942 genes, whereas ZEA was not able to regulate any gene at this level of significance. From this list of 942 upregulated genes, 502 were upregulated more than twofold by EE2-treatment. Although ZEA was able to upregulate 14 genes more than twofold, q values for these genes were all higher than 0.015. EE2 downregulated 2358 genes with $q < 0.001$, from which 798 genes more than twofold. ZEA downregulated 26 genes more than twofold, however, again with $q > 0.001$. Genes that were up- or downregulated by ZEA were all also up- or downregulated by EE2. There was one unknown gene (LOC363386) that was exclusively downregulated 2.1-fold by ZEA (see Supplementary Material, for a complete overview of the gene lists).

Also, the magnitude of regulation was greater for EE2 than for ZEA. The highest concentration of EE2 (10 µg/kg) was able to upregulate 20 genes at least 10-fold. Twenty-five genes were downregulated more than fivefold by 10 µg/kg EE2. Maximal upregulation by ZEA was 6.9-fold, i.e., for matrix metalloproteinase 7 (MMP-7), whereas EE2 upregulated the same gene 381.5-fold. Maximal downregulation by ZEA was 3.6-fold (Gap43), whereas for EE2 it was 8.4-fold (Lrp2) (Supplementary Material).

For both ZEA and EE2, many genes that were regulated at the highest dose levels also showed a dose–response relationship when all the concentrations are taken into account. Although some genes even were differentially expressed at the lowest dose levels of EE2 and ZEA (Table 4), a clear effect of dose on gene expression of most genes is observed at 0.3 µg/kg for EE2 and 0.3 mg/kg ZEA, or higher (for the complete gene list, see Supplementary Material).

Analysis of regulated pathways by the genes identified showed that the main pathways, based on p value of the pathway, that were either positively or negatively affected by EE2 and

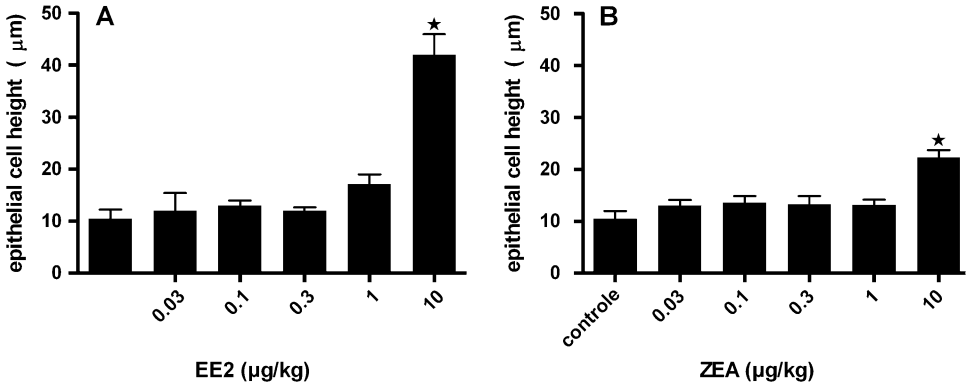

FIG. 2. Uterine epithelial cell height in female Sprague–Dawley rats after a 3-day dietary exposure to EE2 (panel A) and ZEA (panel B). Bars represent averages of four animals and error bars are standard deviations. (*) Significantly different from control ($p < 0.01$).

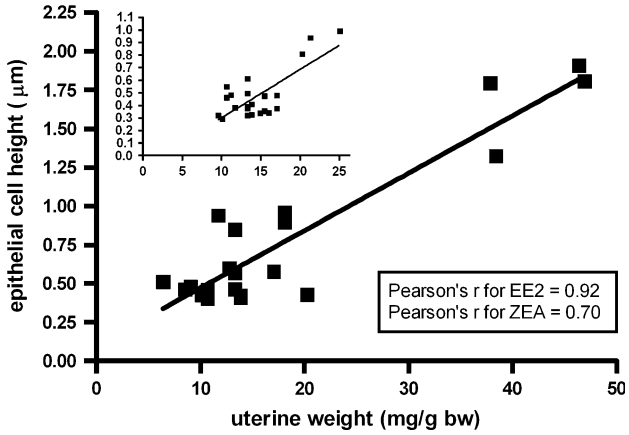

FIG. 3. Pearson's correlation between uterine weight and uterine epithelial cell height in female Sprague–Dawley rats after a 3-day dietary exposure to EE2 or ZEA. Inlay figure is graph for ZEA.

ZEA were inflammation, alternative complement activation, remodeling of extracellular matrix, calcium ion transport, and water homeostasis.

Quantitative RT-PCR

Quantitative RT-PCR was performed with primers representing a selected set of seven genes and used to confirm obtained DNA microarray data. Overall, good agreement was observed between the two methods, although results were more pronounced in the RT-PCR experiments than in the DNA microarray experiments (Table 5).

EE2 and ZEA-Induced Binding Profiles Using Macroarrays with Coregulator-Derived Motifs

Both EE2 and ZEA modulated the binding of ERα-LBD to coregulator-derived motifs in a concentration-dependent manner. Ligand-mediated association, as well as, dissociation of coregulator motifs were observed. For each interaction between EE2- or ZEA-mediated ERα and coregulator motif, the potency (EC_{50}, Fig. 5) and efficacy (Δ-binding, or Y-span between the bottom and top of the curve, Fig. 6) were determined from the concentration–response curve (for individual Δ-binding and concentration–response curves and, see supplemental data). Overall, both ligands modulated the ERα–coregulator interaction in the same qualitative manner, resulting in a similar Δ-binding profile. However, quantitatively, potency as well as efficacy of EE2 was higher than that of ZEA for all interactions.

DISCUSSION

In this study we observed that EE2 has stronger and more potent estrogenic effects than ZEA, based on histology and morphology. With EE2 being a more potent and efficient ERα ligand than ZEA it was hypothesized that EE2 would be a more potent and efficient recruiter of coregulators (both activators and repressors). For the responsive peptides on our chip, EE2 showed a higher potency and efficacy of modulation than ZEA, which was reflected by lower EC_{50} and higher values for Δ-binding for EE2 than for ZEA (Figs. 5 and 6, respectively).

Subsequently, we hypothesized that more potent and efficient coregulator recruitment would result in more potent and efficient modulation of gene transcription levels. In this study, EE2 was able to regulate many more genes than ZEA at much lower doses (efficiency) and to a much higher extent (efficacy) (Table 3).

More pronounced effects on the level of coregulator recruitment and regulation of gene transcription after exposure to EE2 compared to exposure to ZEA suggest that EE2 would exert a more pronounced effect on phenotype, in our case on uterus weight and height of the epithelial layer. The extent of induction of uterine weight after exposure to EE2 was comparable with the observed fourfold increase of blotted uterine weight in immature rats, subcutaneously exposed to different doses up to 10 μg/kg (Naciff *et al*., 2003). Also, a fourfold increase of uterine weight was observed in mice after oral exposure for 3 consecutive days to 100 μg/kg (Fertuck *et al*., 2003; Schmidt *et al*., 2006). Furthermore, subcutaneous exposure of ovariectomized rats to bisphenol A resulted in a maximal fourfold increase of uterine weight (Kanno *et al*., 2003). Where EE2 induced uterine weight 3.8-fold at a dose level of 10 μg/kg, ZEA (10 mg/kg) resulted in a 2.1-fold increase only. Based on a previously performed pilot experiment, in which we used both 10 and 100 μg/kg EE2 and 10 and 100 mg/kg ZEA, we concluded that ZEA is not able to increase uterine weight to the same extent as EE2 (data not published). The LOELs for this endpoint were 1 μg/kg bw and 1 mg/kg bw for EE2 and ZEA, respectively, which are comparable to previously obtained relative potencies for the two compounds (Bovee *et al*., 2004). The maximum increase of epithelial cell height was four- and twofold after exposure to EE2 and ZEA, respectively, which was the same extent of increase as for uterine weight. Plotting uterine weight versus uterine epithelial cell height resulted in a Pearson's correlation $r = 0.89$ (Fig. 3), suggesting a strong correlation between epithelial cell height and uterine weight. However, this observation does not necessarily imply a causal relation between increased epithelial cell height and uterine weight.

In line with the more severe quantitative effects on uterus weight and epithelial cell height, we hypothesized that any other process on the histological level would be more pronounced for EE2 than for ZEA. Surprisingly, the histological coupes revealed a dissimilarity of the appearance of the epithelial layer (Fig. 4). The extensive destruction of the epithelial layer in the ZEA-exposed animals was striking, since in the EE2-exposed animals, the epithelial layer remained intact, despite an increase in thickness.

This observation triggered the hypothesis that EE2 would be more efficient and potent enhancer of transcription of

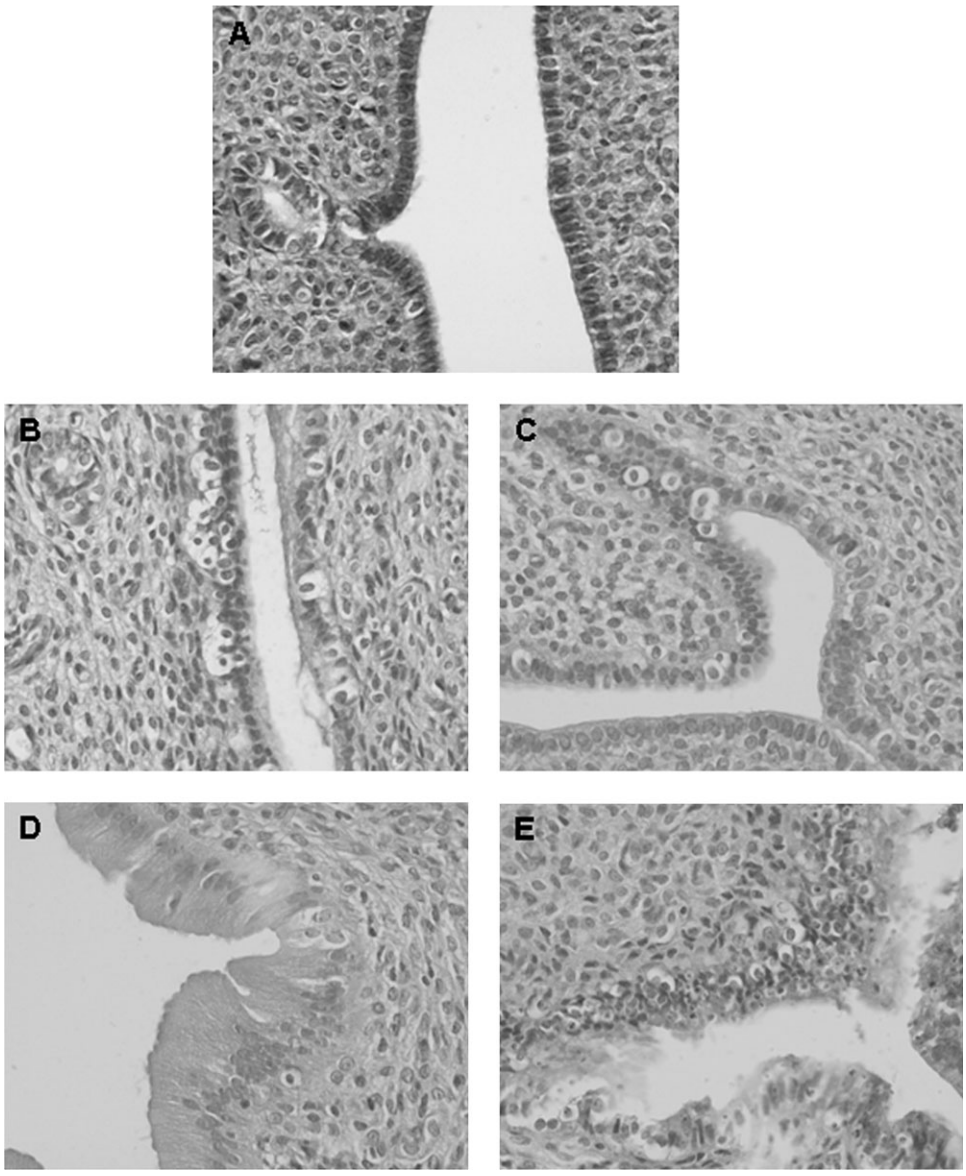

FIG. 4. HE-stained uterus coupes which are representative for the rats of the control and treatment groups. Magnification was ×200. (A) Control animal showing a thin epithelial layer. (B) 0.03 μg/kg EE2: edema and vacuoles. (C) 0.1 mg/kg ZEA: edema and vacuoles. (D) 10 μg/kg EE2: high epithelium. (E) 10 mg/kg ZEA: degenerated epithelium.

anti-inflammatory genes, but analysis of the altered gene expression levels showed that this was not the case.

Inflammation involves the activation of the complement pathway. In our study, many genes involved in this process, such as complement C2, C3, factor B were upregulated by EE2. Overall, we can conclude that the classical and alternative complement activation pathways were both upregulated in rat uterus after exposure to EE2. Interestingly, we observed a far more efficient recruitment of coregulator TRIP9, which is a synonym for inhibitor of kappa B beta (IKBB), by the ERα–EE2 complex than by the ERα–ZEA complex. We hypothesize that IKBB, which is bound to the ER, is not able to sequester NFKB in cytoplasm. Subsequently, enhanced competition of the ERα–EE2 complex and NFKB for IKBB may result in decreased sequestration of NFKB in the cytoplasm, possibly enabling translocation of NFKB to the nucleus and induction of an inflammatory response. We found that EE2 was able to recruit IKBB more efficiently and strongly than ZEA, which is in agreement with a stronger upregulation of inflammatory genes in EE2-treated animals than in ZEA-treated animals. To our knowledge, this is the first time an interaction between ERα and IKBB has been described.

Another pathway that was altered after estrogen exposure was calcium signaling. In epithelial cells, the major role for calcium is the regulation of homeostasis of solutes and water after hormone stimulation (Braun and Schulman, 1995).

TABLE 3
Number of Statistically Significant Changes (FDR, $q < 0.001$) in Gene Expression of at Least Twofold In Uteri of Rats Exposed to Increasing Doses of EE2 or ZEA, Compared to Controls

Treatment	Upregulated	Downregulated
0.03 μg/kg EE2	0	0
0.1 μg/kg EE2	0	1
0.3 μg/kg EE2	1	3
1 μg/kg EE2	16	36
10 μg/kg EE2	502	798
0.03 mg/kg ZEA	0	0
0.1 mg/kg ZEA	0	1
0.3 mg/kg ZEA	0	5
1 mg/kg ZEA	0	3
10 mg/kg ZEA	14	26

TABLE 5
Confirmation of DNA Microarray Data Using Quantitative RT-PCR

	Fold change (microarray)		Fold change (quantitative RT-PCR)	
Gene	EE2	ZEA	EE2	ZEA
APLN	−2.9	−2.3	−17.8	−11.3
AQP5	−7.0	−1.2	−57.8	−2.6
CASP7	2.3	−1.2	3.5	1.1
C2	3.3	1.3	2.7	1.9
MVD	2.3	−1.1	6.6	1.0
SPP	2.7	1.3	22.5	2.9
CALB3	12.4	3.7	21.0	10.9

Note. Fold change of samples from highest dose groups compared to control samples.

Calcium binding protein-9K (CaBP-9K, also Calbindin-3 [Calb-3]) is a calcium ion binding protein that was upregulated up to 12.4-fold and 3.7-fold after exposure to EE2 and ZEA, respectively. Sex steroid hormones and environmental estrogens have been shown to be regulators of Calb-3, suggesting ERα to be a key mediator in the induction of uterine Calb-3 in immature rats (Choi *et al*., 2005). Calb-3 has previously been described as a potent biomarker for estrogen exposure (Lee *et al*., 2005; Naciff *et al*., 2005).

TABLE 4
Dose-Response Effects (Fold Changes Compared with Controls) on Several Genes after Exposure to EE2 and ZEA and Microarray Analysis

			μg/kg EE2				
Gene		RefSeq	0.03	0.1	0.3	1	10
C3	Complement component 3	NM_016994	−1.14	−1.27	1.41	16.73	65.98
Gjb2	Gap junction membrane channel protein beta 2	NM_001004099	−1.08	−1.11	1.22	3.85	38.40
Apln	Apelin	NM_031612	−1.00	−1.22	−1.51	−2.09	−2.89
Calb3	Calbindin-3	NM_012521	1.46	1.47	2.62	9.10	12.41
Gap43	Growth associated protein 43	NM_017195	−0.93	−1.35	−1.87	−3.59	−4.94

			mg/kg ZEA				
Gene		RefSeq	0.03	0.1	0.3	1	10
C3	Complement component 3	NM_016994	−1.61	−1.59	−1.75	−1.30	6.21
Gjb2	Gap junction membrane channel protein beta 2	NM_001004099	−1.12	−1.03	−1.41	−1.09	4.10
Apln	Apelin	NM_031612	−1.10	−1.10	−1.53	−1.61	−2.27
Calb3	Calbindin-3	NM_012521	1.12	0.98	0.93	1.30	3.73
Gap43	Growth associated protein 43	NM_017195	−1.18	−1.13	−1.60	−1.67	−3.58

Water uptake is part of the uterotrophic response after estrogen exposure and aquaporin water channel proteins play a role in many processes as main regulators of membrane osmotic water permeability (King *et al*., 2004). Extracellular hypotonic conditions cause TRPV4 levels to increase, mediating influx of extracellular calcium, subsequently leading to decreased levels of aquaporin 5 (AQP5) (Sidhaye *et al*., 2006). In our study, AQP5 was downregulated sevenfold at the highest tested dose of EE2. Downregulation of AQP5 was also observed by Kwekel *et al*. (2005) following a single oral dose of 100 μg/kg 17α-ethinylestradiol (Kwekel *et al*., 2005).

Water uptake of epithelial cells and subsequent swelling and growth of cells can have serious implications if the cells are not able to expand. Genes involved in the tissue remodeling pathway play an important role in releasing tight junctions and other molecular connections between cells, allowing them to reconfigure and grow without damage. Fluctuations in steroid hormone levels also cause endometrial tissue to go through phases of growth, differentiation, and breakdown in a cyclical manner (Goffin *et al*., 2003). Most matrix-metalloproteinases (MMPs) are involved in the degradation of the extracellular matrix (Marbaix *et al*., 1996) and MMP-7 is predominantly expressed during the proliferative phase of the menstrual cycle (Goffin *et al*., 2003). In our study, MMP-7 gene expression was dramatically upregulated by EE2 (381.4-fold), and to a much smaller extent by ZEA (6.9-fold) at the highest tested doses. Comparable to our results, a 595-fold increase of MMP-7 gene expression in prepubertal uterus and ovaries after exposure to a 4-day dosing regime of 1 μg 17α-ethynylestradiol/kg bw/day, administered by subcutaneous injection, was previously observed (Naciff *et al*., 2005), suggesting an important role of MMP-7 in estrogen-induced

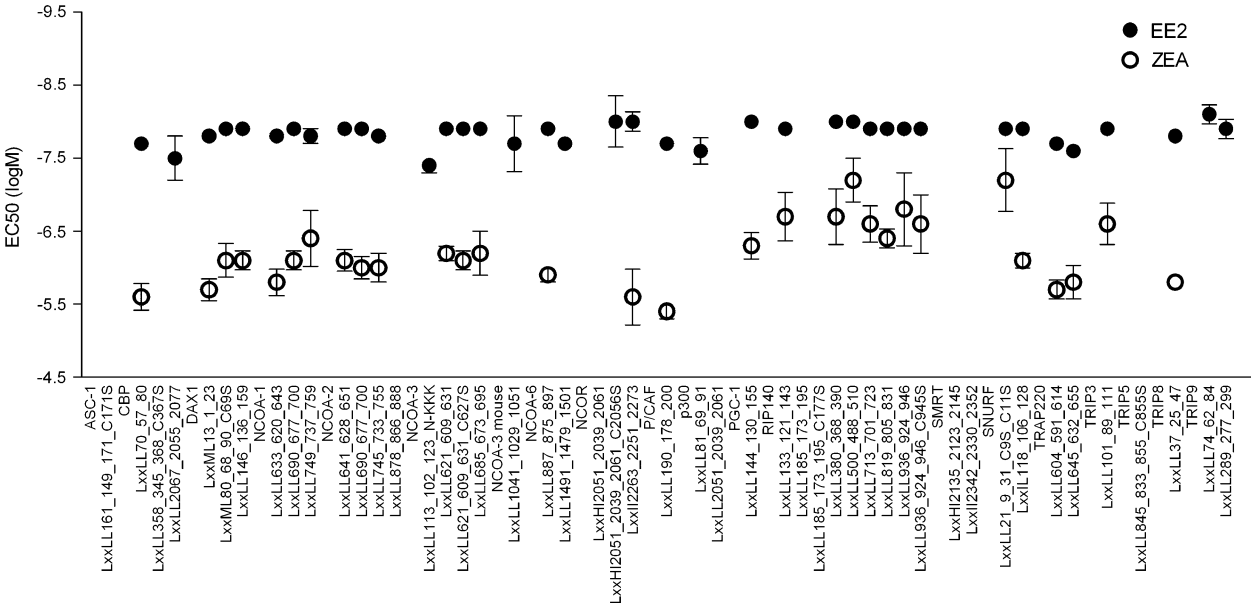

FIG. 5. Profile of EC_{50} values ± standard deviations of EE2- and ZEA-induced modulation of ERα-peptide interaction.

proliferation of the endometrium. Secreted phosphoprotein 1 (spp1), or osteopontin, is an adhesion molecule that plays a role in extracellular matrix reorganization and it is upregulated in all pregnant mammalian uteri, which have been studied so far (Liaw *et al.*, 1998; White *et al.*, 2005). Spp1 has been identified as a substrate for MMP-7 (Yu *et al.*, 2002). Daston and Naciff (2005) indicated that exposure to EE2 (1–10 μg/kg/day) resulted in upregulation of MMP-7 and downregulation of spp1 in the reproductive system of the immature rat, assuming that the net effect would lead to an increase of uterine weight. In our study, however, MMP-7, as well as spp1 (2.7-fold), was upregulated at the highest tested dose of EE2 suggesting a cooperative manner of increasing uterine weight. Spp1 is also thought to play a role in an antiapoptotic pathway and in inflammation.

As described above, EE2 increases binding of ERα to IKBB, possibly indirectly activating nuclear factor kappa beta (NFKB) and NFKB/AP1 (activating protein-1)-responsive genes, such

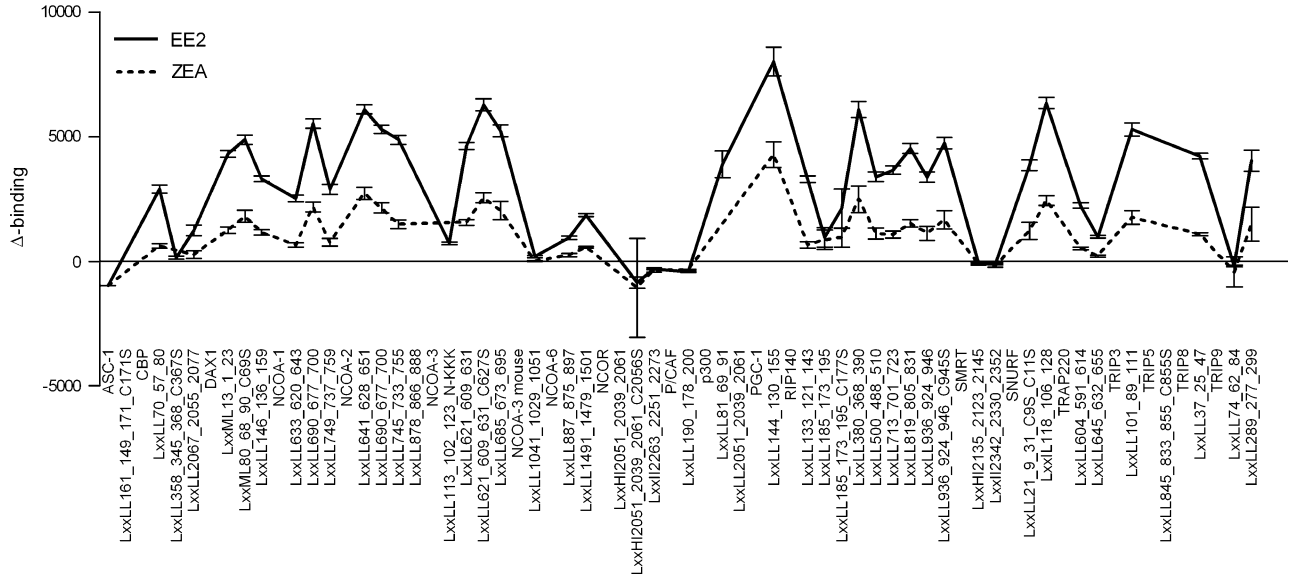

FIG. 6. Profile of delta-binding ± standard deviations (arbitrary units) of EE2- and ZEA-induced modulation of ERα-peptide interaction. Delta binding was defined as the absolute difference between top and bottom values of the fitted sigmoidal dose–response curve.

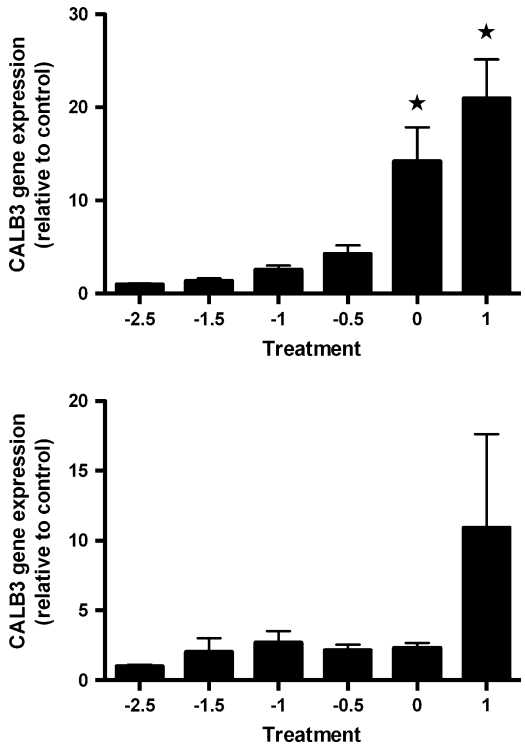

FIG. 7. Relative gene expression levels of CALB3 using quantitative RT-PCR, relative to control group (set at −2.5). Upper panel: Animals were treated with EE2 (0–10μM). Lower panel: Animals were treated with ZEA (0–10mM). Bars are averages of two animals measured in duplo. Error bars are standard errors of the mean. (*) Represents statistically significant from control group ($p < 0.05$).

as MMP-7 (Fernandez-Figueras *et al.*, 2006; Holnthoner *et al.*, 2006). Furthermore, estrogens have been described to decrease tight junctional resistance by MMP-7–mediated remodeling of occludin, possible allowing for harmless cell growth (Gorodeski, 2007).

The much higher efficiency of the EE2–ERα complex compared to ZEA–ERα complex to recruit IKBB, in combination with the dramatic increase in MMP-7 gene expression after EE2 exposure as compared with the increase after ZEA exposure, suggests that the observed differences in uterine tissue damage at the histological level could be caused by differential abilities to respond to tissue-remodeling processes in order to cope with estrogen-induced increases of water uptake and cell growth.

The present study also aimed to examine whether dietary exposure of rats to either EE2 or ZEA would lead to dose-dependent and compound-specific effects in the reproductive tract. Results point in the direction of qualitatively similar gene expression profiles for EE2 and ZEA. However, the level of regulation clearly differed between the two, attributing a much lower estrogenic potency to ZEA than to EE2. It was previously suggested that the synthetic estrogen diethylstilltestrol (DES) and the phytoestrogen genistein operate via a molecular mechanism analogous to that of the endogenous estrogen (E2) in the rodent uterus (Moggs *et al.*, 2004). Additionally, Watanabe (2003) described a dose-dependent activation and repression of estrogen-related gene expression. In their paper, they state that endogenous and xenobiotic estrogens do not exert identical effects on uterine gene expression. However, in their study, E2 and DES induced many genes to respond in the same way, but different groups of genes showed varying levels of maximal activities to each estrogen, resulting in different dose–response patterns. The differences in gene expression patterns of the two estrogens, thus mainly reflect a difference in relative potency of each estrogen, which may also be the case for our study. The same phenomenon was observed in a study with nonylphenol and E2 in which high doses of nonylphenol were able to activate all genes activated by E2, whereas lower doses of nonylphenol had little effect on the genes that were activated by E2 (Watanabe *et al.*, 2004).

Furthermore, we postulated that changes in gene expression patterns may potentially serve as a more reliable indicator for effects at the low end of the dose–response curve (Daston and Naciff, 2005) and they may be used as additional toxicological parameters in hazard identification and quantitative, mechanistic-based risk assessments (Naciff and Daston, 2004). Therefore, we aimed to identify the lowest exposure level that results in changes in gene expression levels in an attempt to identify sensitive molecular biomarkers for compound-specific estrogenic effects. Regulations at these exposure levels are often rather small, but we considered them to be relevant if they were part of a dose-dependent response when the other dose levels were also taken into account. Table 4 lists a number of genes, such as AQP5 and Calb3 that were regulated after exposure to low doses of EE2 or ZEA. Therefore, they potentially could serve as sensitive biomarkers for *in vivo* estrogen exposure (Fig. 7). Future studies imply inclusion of treatment doses which are closer to human exposure levels, in order to better assess the risk of dietary exposure to estrogenic compounds.

SUPPLEMENTARY DATA

Supplementary data are available online at http://toxsci.oxfordjournals.org/.

ACKNOWLEDGMENTS

The authors thank Dr. Michel Nielen, Dr. Ron Hoogenboom, and Dr. Evert van Schothorst for careful reading of the manuscript. Hakan Baykus, Dirk Pijnenburg, and Diana Melchers are acknowledged for their technical support.

REFERENCES

Benjamini, Y., and Hochberg, Y. (1995). Controlling the false discovery rate—A practical and powerful approach to multiple testing. *J.R. Stat. Soc. Ser. B Methodol.* **57,** 289–300.

Bovee, T. F. H., Helsdingen, R. J. R., Rietjens, I. M. C. M., Keijer, J., and Hoogenboom, R. L. A. P. (2004). Rapid yeast estrogen bioassays stably expressing human estrogen receptors [alpha] and [beta], and green fluorescent protein: A comparison of different compounds with both receptor types. *J. Steroid Biochem. Mol. Biol.* **91,** 99–109.

Braun, A. P., and Schulman, H. (1995). The multifunctional calcium/calmodulin-dependent protein kinase: From form to function. *Annu. Rev. Physiol.* **57,** 417–445.

Choi, K. C., Leung, P. C. K., and Jeung, E. B. (2005). Biology and physiology of Calbindin-D9k in female reproductive tissues: Involvement of steroids and endocrine disruptors. *Reprod. Biol. Endocrinol.* **3,** 66.

Currie, R. A., Orphanides, G., and Moggs, J. G. (2005). Mapping molecular responses to xenoestrogens through Gene Ontology and pathway analysis of toxicogenomic data. *Reprod. Toxicol.* **20,** 433–440.

Daston, G. P., and Naciff, J. M. (2005). Gene expression changes related to growth and differentiation in the fetal and juvenile reproductive system of the female rat: Evaluation of microarray results. *Reprod. Toxicol.* **19,** 381–394.

Edwards, D. P. (2000). The role of coactivators and corepressors in the biology and mechanism of action of steroid hormone receptors. *J. Mamm. Gland Biol. Neoplasia* **5,** 307–324.

Eriksen, G. S., Pennington, J., and Schlatter, J. (2000). Safety evaluation of certain food additives and contaminants. *WHO Food Addit. Ser.* **44,** 393–482.

Fernandez-Figueras, M.-T., Puig, L., Musulen, E., Gilaberte, M., Lerma, E., Serrano, S., Ferrandiz, C., and Ariza, A. (2006). Expression profiles associated with aggressive behavior in Merkel cell carcinoma. *Mod. Pathol.* **20,** 90–101.

Fertuck, K. C., Eckel, J. E., Gennings, C., and Zacharewski, T. R. (2003). Identification of temporal patterns of gene expression in the uteri of immature, ovariectomized mice following exposure to ethynylestradiol. *Physiol. Genomics* **15,** 127–141.

Goffin, F., Munaut, C., Frankenne, F., Perrier d'Hauterive, S., Beliard, A., Fridman, V., Nervo, P., Colige, A., and Foidart, J.-M. (2003). Expression pattern of metalloproteinases and tissue inhibitors of matrix-metalloproteinases in cycling human endometrium. *Biol. Reprod.* **69,** 976–984.

Gorodeski, G. I. (2007). Estrogen decrease in tight junctional resistance involves matrix-metalloproteinase-7-mediated remodeling of occludin. *Endocrinology* **148,** 218–231.

Hall, J. M., Couse, J. F., and Korach, K. S. (2001). The multifaceted mechanisms of estradiol and estrogen receptor signaling. *J. Biol. Chem.* **276,** 36869–36872.

Holnthoner, W., Kerenyi, M., Groger, M., Kratochvill, F., and Petzelbauer, P. (2006). Regulation of matrilysin expression in endothelium by fibroblast growth factor-2. *Biochem. Biophys. Res. Commun.* **342,** 725–733.

Kanno, J., Onyon, L., Peddada, S., Ashby, J., Jacob, E., and Owens, W. (2003). The OECD program to validate the rat uterotrophic bioassay. Phase 2: Dose-response studies. *Environ. Health Perspect.* **111,** 1530–1549.

Katzenellenbogen, J. A., O'Malley, B. W., and Katzenellenbogen, B. S. (1996). Tripartite steroid hormone receptor pharmacology: Interaction with multiple effector sites as a basis for the cell- and promoter-specific action of these hormones. *Mol. Endocrinol.* **10,** 119–131.

King, L. S., Kozono, D., and Agre, P. (2004). From structure to disease: The evolving tale of aquaporin biology. *Nat. Rev. Mol. Cell Biol.* **5,** 687–698.

Klinge, C. M. (2001). Estrogen receptor interaction with estrogen response elements. *Nucleic Acids Res.* **29,** 2905–2919.

Kuiper, G. G. J. M., Shughrue, P. J., Merchenthaler, I., and Gustafsson, J.-A. (1998). The estrogen receptor [beta] subtype: A novel mediator of estrogen action in neuroendocrine systems. *Front. Neuroendocrinol.* **19,** 253–286.

Kwekel, J. C., Burgoon, L. D., Burt, J. W., Harkema, J. R., and Zacharewski, T. R. (2005). A cross-species analysis of the rodent uterotrophic program: Elucidation of conserved responses and targets of estrogen signaling. *Physiol. Genomics* **23,** 327–342.

Lee, G.-S., Kim, H.-J., Jung, Y.-W., Choi, K.-C., and Jeung, E.-B. (2005). Estrogen receptor {alpha} pathway is involved in the regulation of calbindin-D9k in the uterus of immature rats. *Toxicol. Sci.* **84,** 270–277.

Liaw, L., Birk, D. E., Ballas, C. B., Whitsitt, J. S., Davidson, J. M., and Hogan, B. L. (1998). Altered wound healing in mice lacking a functional osteopontin gene (spp1). *J. Clin. Invest.* **101,** 1468–1478.

Lonard, D. M., and O'Malley, B. W. (2006). The expanding cosmos of nuclear receptor coactivators. *Cell* **125,** 411–414.

Lone, K. P. (1997). Natural sex steroids and their xenobiotic analogs in animal production: Growth, carcass quality, pharmacokinetics, metabolism, mode of action, residues, methods, epidemiology. *Crit. Rev. Food Sci. Nutr.* **37,** 93–209.

Marbaix, E., Kokorine, I., Moulin, P., Donnez, J., Eeckhout, Y., and Courtoy, P. J. (1996). Menstrual breakdown of human endometrium can be mimicked in vitro and is selectively and reversibly blocked by inhibitors of matrix metalloproteinases. *Proc. Natl. Acad. Sci. U.S.A.* **93,** 9120–9125.

McDonnel, D. P., and Norris, J. D. (1997). Analysis of the molecular pharmacology of estrogen receptor agonists and antagonists provide insights into the mechanisms of estrogen in bone. *Osteoporos. Int.* **7,** S29–S34.

Meyer, H. H. (2001). Biochemistry and physiology of anabolic hormones used for improvement of meat production. *APMIS* **109,** 1–8.

Minervini, F., Giannoccaro, A., Cavallini, A., and Visconti, A. (2005). Investigations on cellular proliferation induced by zearalenone and its derivatives in relation to the estrogenic parameters. *Toxicol. Lett.* **159,** 272–283.

Moggs, J. G., Ashby, J., Tinwell, H., Lim, F. L., Moore, D. J., Kimber, I., and Orphanides, G. (2004). The need to decide if all estrogens are intrinsically similar. *Environ. Health Perspect.* **112,** 1137–1142.

Naciff, J. M., and Daston, G. P. (2004). Toxicogenomic approach to endocrine disrupters: Identification of a transcript profile characteristic of chemicals with estrogenic activity. *Toxicol. Pathol.* **32,** 59–70.

Naciff, J. M., Overmann, G. J., Torontali, S. M., Carr, G. J., Tiesman, J. P., Richardson, B. D., and Daston, G. P. (2003). Gene expression profile induced by 17{alpha}-ethynyl estradiol in the prepubertal female reproductive system of the rat. *Toxicol. Sci.* **72,** 314–330.

Naciff, J. M., Torontali, S. M., Overmann, G. J., Carr, G. J., Tiesman, J. P., and Daston, G. P. (2005). Evaluation of the gene expression changes induced by 17-alpha-ethynyl estradiol in the immature uterus/ovaries of the rat using high density oligonucleotide arrays. *Birth Defects Res. B* **74,** 164–184.

Nettles, K. W., and Greene, G. L. (2005). Ligand control of coregulator recruitment to nuclear receptors. *Annu. Rev. Physiol.* **67,** 309–333.

Nilsson, S., Makela, S., Treuter, E., Tujague, M., Thomsen, J., Andersson, G., Enmark, E., Pettersson, K., Warner, M., and Gustafsson, J.-A. (2001). Mechanisms of estrogen action. *Physiol. Rev.* **81,** 1535–1565.

Nuwaysir, E. F., Bittner, M., Trent, J., Barrett, J. C., and Afshari, C. A. (1999). Microarrays and toxicology: The advent of toxicogenomics. *Mol. Carcinogenesis* **24,** 153–159.

Pellis, L., Franssen-van Hal, N. L. W., Burema, J., and Keijer, J. (2003). The intraclass correlation coefficient applied for evaluation of data correction, labeling methods, and rectal biopsy sampling in DNA microarray experiments. *Physiol. Genomics* **16,** 99–106.

Schmidt, S., Degen, G., Seibel, J., Hertrampf, T., Vollmer, G., and Diel, P. (2006). Hormonal activity of combinations of genistein, bisphenol A and 17-beta estradiol in the female Wistar rat. *Arch. Toxicol.* **80,** 839–845.

Sidhaye, V. K., Guler, A. D., Schweitzer, K. S., D'Alessio, F., Caterina, M. J., and King, L. S. (2006). Transient receptor potential vanilloid 4 regulates aquaporin-5 abundance under hypotonic conditions. *Proc. Natl. Acad. Sci. U.S.A.* **103,** 4747–4752.

Steiner, S., and Anderson, N. L. (2000). Expression profiling in toxicology—Potentials and limitations. *Toxicol. Lett.* **112–113,** 467–471.

Wang, H., Masironi, B., Eriksson, H., and Sahlin, L. (1999). A comparative study of estrogen receptors {alpha} and {beta} in the rat uterus. *Biol. Reprod.* **61,** 955–964.

Watanabe, H., Suzuki, A., Goto, M., Lubahn, D., Handa, H., and Iguchi, T. (2004). Tissue-specific estrogenic and non-estrogenic effects of a xenoestrogen, nonylphenol. *J. Mol. Endocrinol.* **33,** 243–252.

Watanabe, H., Suzuki, A., Kobayashi, M., Lubahn, D., Handa, H., and Iguchi, T. (2003). Similarities and differences in uterine gene expression patterns caused by treatment with physiological and non-physiological estrogens. *J. Mol. Endocrinol.* **31,** 487–497.

White, F. J., Ross, J. W., Joyce, M. M., Geisert, R. D., Burghardt, R. C., and Johnson, G. A. (2005). Steroid regulation of cell specific secreted phosphoprotein 1 (Osteopontin) expression in the pregnant porcine uterus. *Biol. Reprod.* **73,** 1294–1301.

Yu, W.-H., Woessner, J. F., Jr, McNeish, J. D., and Stamenkovic, I. (2002). CD44 anchors the assembly of matrilysin/MMP-7 with heparin-binding epidermal growth factor precursor and ErbB4 and regulates female reproductive organ remodeling. *Genes Dev.* **16,** 307–323.